*Journal of Engineering Physics and Thermophysics, Vol. 82, No. 5, 2009*

# EFFECTS OF MASS TRANSFER ON FREE CONVECTION FLOW PAST A SEMI-INFINITE INCLINED PLATE WITH VARIABLE SURFACE TEMPERATURE

**G. Palani and Kwang-Yong Kim**

UDC 536.25

*The unsteady free convection flow past a semi-infinite inclined plate with a variable surface temperature and mass flux is considered. The governing unsteady, two-dimensional, coupled, nonlinear integrodifferential equations are transformed into a set of non- dimensional equations that are solved numerically using an implicit finite-difference method. A representative set of the results obtained is displayed graphically to illustrate the influence of various physical parameters on the velocity, temperature, and concentration profiles. The local and average skin friction, Nusselt number, and Sherwood number are also presented.*

***Keywords****: Inclined plate, Nusselt number, skin friction, Sherwood number, finite difference.*

**Introduction.** Free convection flow frequently occurs in nature. Free convection takes place not only due to temperature difference, but also due to concentration differences or a combination of both. The study of convection with both heat and mass transfer is very useful in various fields such as industry, agriculture, and oceanography. Representative fields of interest, where combined heat and mass transfer plays an important role, are design of chemical processing equipment, formation and dispersion of fog, distribution of temperature and moisture over agricultural fields and groves of fruit trees, damage of crops due to freezing, and pollution of the environment.

The steady-state problem of simultaneous heat and mass transfer by free convection about a vertical plate with uniform surface temperature and concentration was solved by Somers [1] and Wilcox [2] using an integral method. Gebhart and Pera [3] obtained the steady-state solution for natural convection on a vertical plate with variable surface temperature and mass diffusion using similarity variables. Callahan and Marner [4] gave a numerical solution for the problem of transient free convection with mass transfer on an isothermal vertical flat plate by employing an explicit finite difference scheme. Soundalgekar and Ganesan [5] solved the problem of transient free convection with mass transfer on a vertical plate with a constant heat flux by using an implicit finite difference scheme. Ekambavannan and Ganesan [6] studied unsteady natural convection flow along an inclined plate with variable surface temperature and mass diffusion by employing an implicit finite difference scheme. In nature, the mass may be diffused from the surface at a constant rate. However, the problem of natural convection flow over an inclined plate with variable surface temperature and mass flux did not receive the attention of researchers. Hence, it is now proposed to solve such an unsteady problem.

**Mathematical Analysis.** A problem of two-dimensional, unsteady, laminar free convection flow past a semi-infinite inclined plate of a viscous incompressible fluid with variable surface temperature and mass flux is formulated mathematically. It is assumed that the concentration $C'$ of the diffusing species in a binary mixture is very low in comparison to the other. This leads to the assumption that the Soret and Dufor effects are negligible. It is also assumed that the effect of viscous dissipation is negligible in the energy equation and there is no chemical reaction between the fluid and diffusing species.

The angle of inclination of the plate to the horizontal is assumed to be $\phi$. The $x$ and $y$ axes are directed along the plate and upward normal to it. It is assumed that initially the plate and the fluid are at the same temperature and the fluid is characterized by a constant concentration. At time $t' \geq 0$ the temperature near the plate is raised to $T'_w(x) = T'_\infty + ax^n$, mass is supplied from the plate to the fluid at the rate $q_w(x) = bx^m$, and further they are maintained as such. Then, under the usual Boussinesq approximation, the boundary layer flow is governed by the following equations:

Department of Mechanical Engineering, Inha University, Incheon 402-751, Republic of Korea; email: gpalani32@yahoo.co.in. Published in Inzhenerno-Fizicheskii Zhurnal, Vol. 82, No. 5, pp. 869–878, September–October, 2009. Original article submitted May 8, 2008; revision submitted December 22, 2008.

 

$$\frac{\partial u}{\partial x}+\frac{\partial v}{\partial y}=0\,, \tag{1}$$

$$\frac{\partial u}{\partial t'}+u\frac{\partial u}{\partial x}+v\frac{\partial u}{\partial y}=g\beta\cos\phi\,\frac{\partial}{\partial x}\int_y^\infty\left(T'-T'_\infty\right)dy+g\beta^*\cos\phi\,\frac{\partial}{\partial x}\int_y^\infty\left(C'-C'_\infty\right)dy$$

$$+g\beta\sin\phi\left(T'-T'_\infty\right)+g\beta^*\sin\phi\left(C'-C'_\infty\right)+\nu\frac{\partial^2 u}{\partial y^2}\,, \tag{2}$$

$$\frac{\partial T'}{\partial t'}+u\frac{\partial T'}{\partial x}+v\frac{\partial T'}{\partial y}=\alpha\frac{\partial^2 T'}{\partial y^2}\,, \tag{3}$$

$$\frac{\partial C'}{\partial t'}+u\frac{\partial C'}{\partial x}+v\frac{\partial C'}{\partial y}=D\frac{\partial^2 C'}{\partial y^2}\,. \tag{4}$$

The initial and boundary conditions are as follows:

$$t'\le 0:\ \ u=0\,,\ \ v=0\,,\ \ T'=T'_\infty\,,\ \ C'=C'_\infty\,;$$

$$t'>0:\ \ u=0\,,\ \ v=0\,,\ \ T'_{\mathrm{w}}(x)=T'_\infty+ax^n\,,\ \ \frac{\partial C'}{\partial y}=-\frac{q_{\mathrm{w}}(x)}{D}\ \text{ at }\ y=0\,,$$

$$u=0\,,\ \ T'=T'_\infty\,,\ \ C'=C'_\infty\ \text{ at }\ x=0\,,$$

$$u\to 0\,,\ \ T'\to T'_\infty\,,\ \ C'\to C'_\infty\ \text{ as }\ y\to\infty\,, \tag{5}$$

where $q_{\mathrm{w}}(x) = bx^m$. Introducing nondimensional quantities

$$X=\frac{x}{L}\,,\ \ Y=\frac{y}{L}\,\mathrm{Gr}^{1/4}\,,\ \ U=\frac{uL}{\nu}\,\mathrm{Gr}^{-1/2}\,,\ \ V=\frac{vL}{\nu}\,\mathrm{Gr}^{-1/4}\,,$$

$$t=\frac{\nu t'}{L^2}\,\mathrm{Gr}^{1/2}\,,\ \ T=\frac{T'-T'_\infty}{T'_{\mathrm{w}}(L)-T'_\infty}\,,\ \ C=\frac{C'-C'_\infty}{q_{\mathrm{w}}(L)\,L/D}\,\mathrm{Gr}^{1/4}\,,$$

$$\mathrm{Gr}=\frac{g\beta L^3\left(T'_{\mathrm{w}}(L)-T'_\infty\right)}{\nu^2}\,,\ \ \mathrm{Gc}=\frac{g\beta^* L^4 q_{\mathrm{w}}}{\nu^2 D}\,,$$

$$\mathrm{Pr}=\frac{\nu}{\alpha}\,,\ \ \mathrm{Sc}=\frac{\nu}{D}\,,\ \ N=\frac{\mathrm{Gc}}{\mathrm{Gr}}\,, \tag{6}$$

we reduce the governing equations to the following form:

$$\frac{\partial U}{\partial X}+\frac{\partial V}{\partial Y}=0\,, \tag{7}$$

$$\frac{\partial U}{\partial t}+U\frac{\partial U}{\partial X}+V\frac{\partial U}{\partial Y}=\mathrm{Gr}^{-1/4}\cos\phi\,\frac{\partial}{\partial X}\int_Y^\infty T\,dY+N\,\mathrm{Gr}^{-1/2}\cos\phi\,\frac{\partial}{\partial X}\int_Y^\infty C\,dY$$

$$+T\sin\phi+N\,\mathrm{Gr}^{-1/4}\,C\sin\phi+\frac{\partial^2 U}{\partial Y^2}, \tag{8}$$

$$\frac{\partial T}{\partial t}+U\frac{\partial T}{\partial X}+V\frac{\partial T}{\partial Y}=\frac{1}{\mathrm{Pr}}\frac{\partial^2 T}{\partial Y^2}, \tag{9}$$

$$\frac{\partial C}{\partial t}+U\frac{\partial C}{\partial X}+V\frac{\partial C}{\partial Y}=\frac{1}{\mathrm{Sc}}\frac{\partial^2 C}{\partial Y^2}. \tag{10}$$

The corresponding nondimensional initial and boundary conditions are given by

$$t\le 0:\ U=0,\ V=0,\ T=0,\ C=0;$$

$$t>0:\ U=0,\ V=0,\ T=X^n,\ \frac{\partial C}{\partial Y}=-X^m\ \text{ at }\ Y=0,$$

$$U=0,\ T=0,\ C=0\ \text{ at }\ X=0,$$

$$U\to 0,\ T\to 0,\ C\to 0\ \text{ as }\ Y\to\infty. \tag{11}$$

The local and average nondimensional skin friction, Nusselt number, and Sherwood number are

$$\bar{\tau}_x=\mathrm{Gr}^{3/4}\left.\frac{\partial U}{\partial Y}\right|_{Y=0}, \tag{12}$$

$$\bar{\tau}=\mathrm{Gr}^{3/4}\int_0^1\left.\frac{\partial U}{\partial Y}\right|_{Y=0}dX, \tag{13}$$

$$\mathrm{Nu}_X=-X\,\mathrm{Gr}^{1/4}\frac{\left.\frac{\partial T}{\partial Y}\right|_{Y=0}}{T|_{Y=0}}, \tag{14}$$

$$\overline{\mathrm{Nu}}=-\,\mathrm{Gr}^{1/4}\int_0^1\frac{\left.\frac{\partial T}{\partial Y}\right|_{Y=0}}{T|_{Y=0}}dX, \tag{15}$$

$$\mathrm{Sh}_X=-X\,\mathrm{Gr}^{1/4}\frac{\left.\frac{\partial C}{\partial Y}\right|_{Y=0}}{C|_{Y=0}}, \tag{16}$$

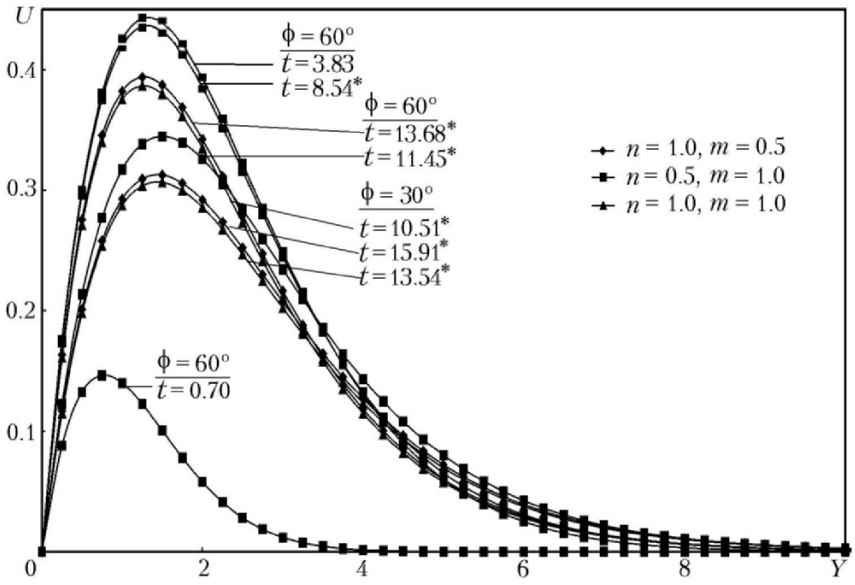


Fig. 1. Transient velocity profiles at $X = 1$, Pr = 0.7, Sc = 0.5, Gr = $10^6$, $N = 1$ for different values of ϕ, $n$, and $m$. Hereinafter, the asterisk corresponds to a steady state.

$$\overline{\mathrm{Sh}} = -\,\mathrm{Gr}^{1/4} \int_0^1 \frac{\left.\dfrac{\partial C}{\partial Y}\right|_{Y=0}}{C\big|_{Y=0}}\, dX\,. \tag{17}$$

**Numerical Technique.** The unsteady, nonlinear, coupled integrodifferential equations (7)–(10) with the initial and boundary conditions (11) are solved by employing a finite difference scheme of Crank–Nicholson type. The finite difference equations corresponding to the equations mentioned above, and the procedure of calculation are analogous to those presented in [7]. In particular, the equations for concentration constitute a tri-diagonal system of equations that are solved by the Thomas algorithm described by Carnahan et al. [8].

**Results and Discussion.** Temporal maximum and steady-state velocity profiles are given in Fig. 1. This figure shows the effect of inclination angle ϕ and exponents $n$ and $m$ on velocity $U$. When ϕ is reduced, the normal component of the combined buoyancy force increases near the leading edge, which causes an impulsive driving force for the fluid motion along the plate. The temperature gradient and mass flux along the plate near the leading edge vary inversely with $n$ and $m$, respectively. Due to these facts, the impulsive force along the plate increases with decreasing value of each of ϕ, $n$, and $m$. Since the tangential component of the buoyancy force that dominates in the downstream increases with ϕ, maximum velocity increases therewith too. The increase in the value of $n$ or $m$ reduces the temperature and concentration on the surface, respectively, up to $X = 1.0$. Therefore, the velocity decreases with increasing value of either $n$ or $m$, and the effect of $n$ is more significant.

Transient velocity profiles are given in Fig. 2, which shows the effect of the buoyancy force ratio $N$ and Grashof number Gr on velocity. The velocity increases with $N$, but decreases with increasing value of Gr. This indicates that the buoyancy force due to concentration dominates over the thermal buoyancy force in the region near the plate. The mentioned forces are opposite when $N$ is negative, and due to their interaction the time taken to reach the steady state is longer.

Temporal maximum and steady-state temperature distributions are given in Fig. 3 for different values of $n$ and ϕ. It is observed that the temperature increases steadily in the transient period and reaches the steady-state value. A lower temperature is seen for a system with higher values of ϕ or $n$. It is also shown that the system reaches the steady state earlier when $n$ is small. The effect of the exponent $n$ on the temperature profile is absent for small times.

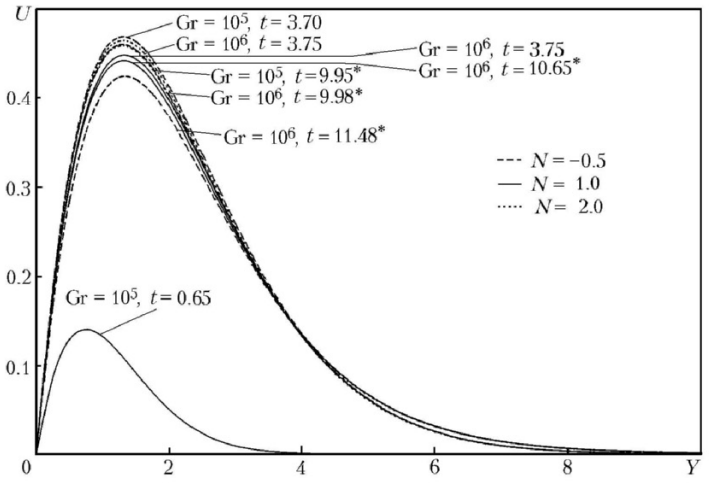


Fig. 2. Transient velocity profiles at $X$ = 1, Pr = 0.7, Sc = 0.5, $\phi$ = 60°, $n$ = 0.5, $m$ = 0.5 for different values of Gr and $N$.

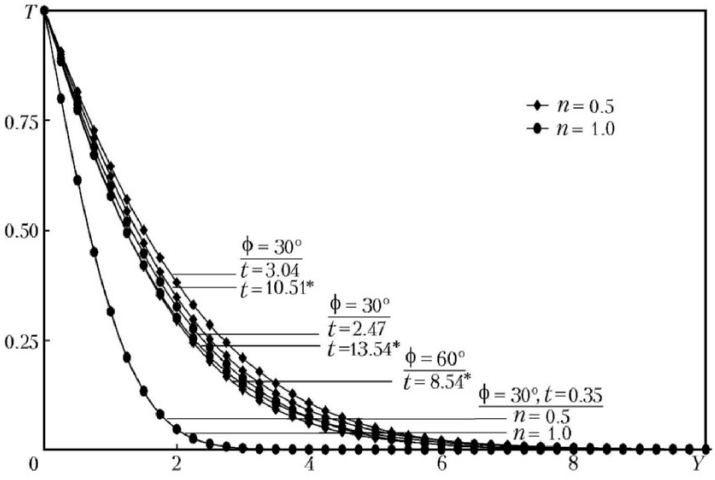


Fig. 3. Transient temperature profiles at $X$ = 1, Pr = 0.7, Sc = 0.5, Gr = $10^6$, $N$ = 1, $m$ = 1 for different values of $n$ and $\phi$.

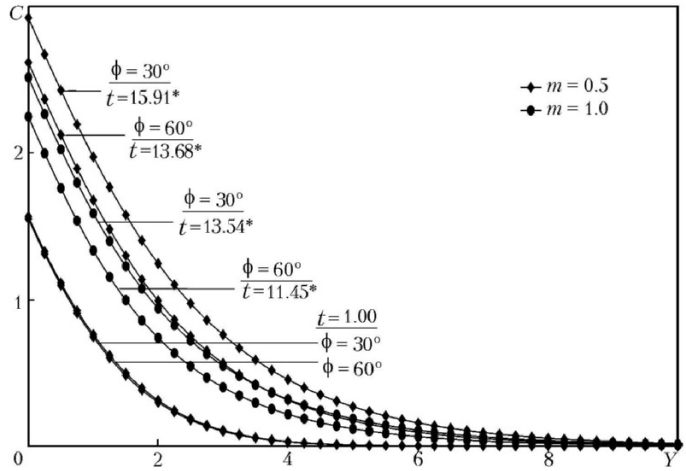


Fig. 4. Transient concentration profiles at $X$ = 1, Pr = 0.7, Sc = 0.5, Gr = $10^6$, $N$ = 1, $n$ = 1 for different values of $m$ and $\phi$.

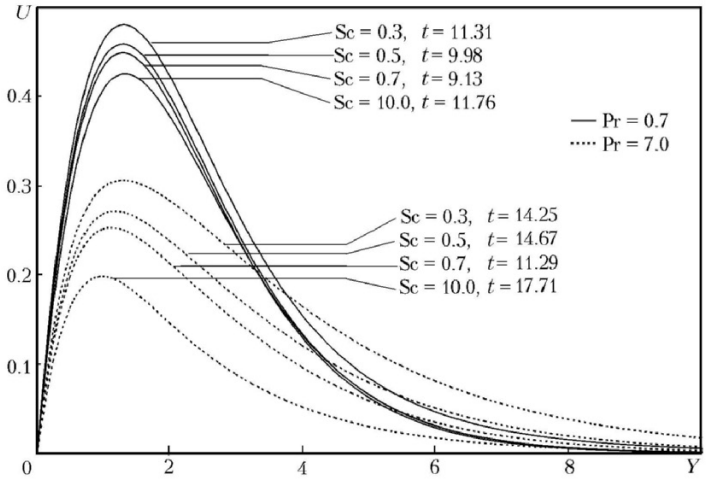


Fig. 5. Steady-state velocity profiles at $X = 1$, Gr = $10^6$, $N = 2$, $\phi = 60^o$, $n = 0.5$, $m = 0.5$ for different values of Pr and Sc.

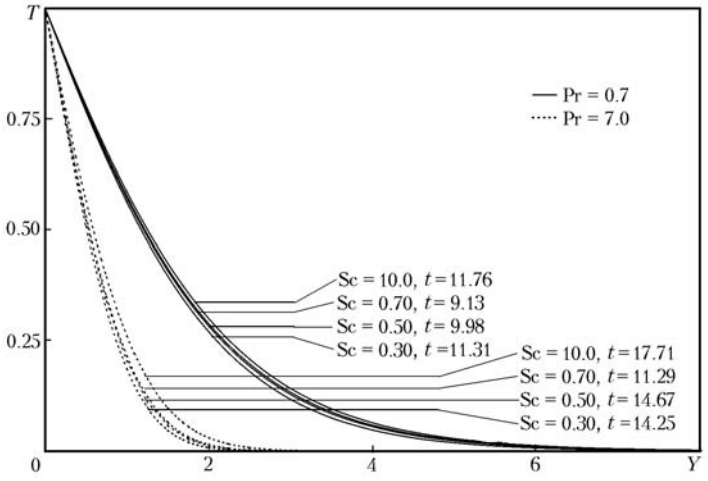


Fig. 6. Steady-state temperature profiles at $X = 1$ for different values of Pr and Sc. The values of the quantities are same as in Fig. 5.

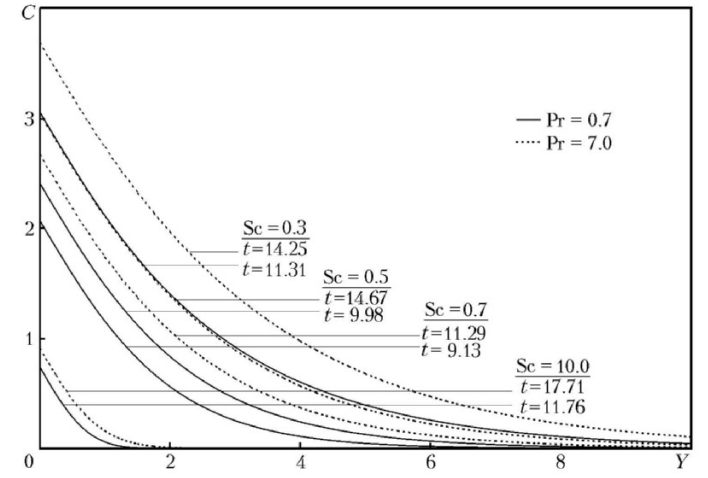


Fig. 7. Steady-state concentration profiles at $X = 1$ for different values of Pr and Sc. The values of the quantities are same as in Fig. 5.

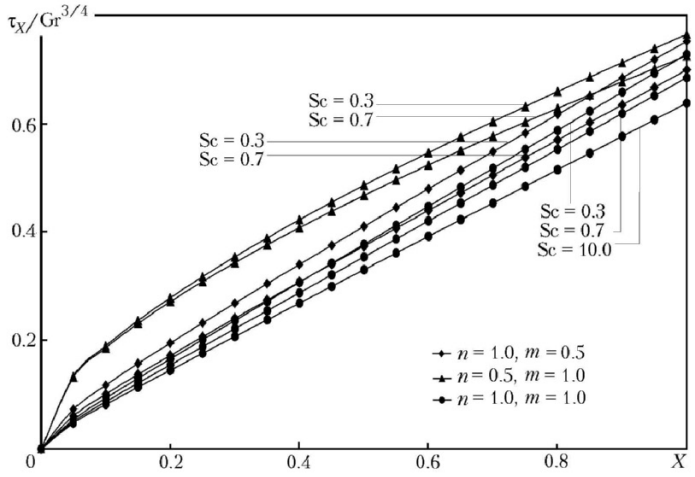


Fig. 8. Local skin friction at Gr = $10^6$, $N = 2$, $\phi = 45^o$, Pr = 0.7 for different values of Sc, $n$, and $m$.

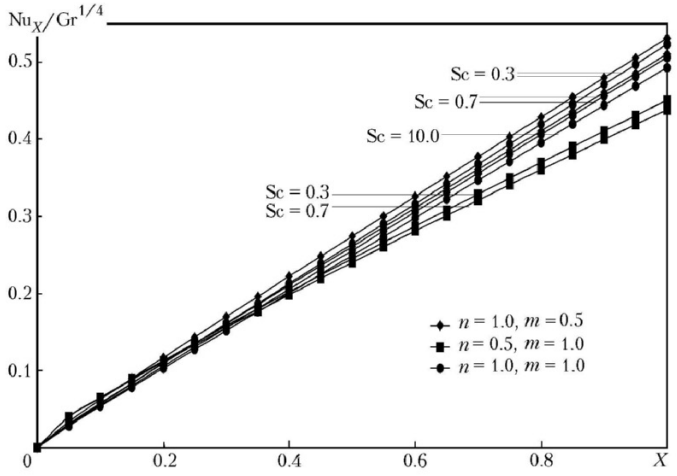


Fig. 9. Local Nusselt number for different values of Sc, $n$, and $m$. The values of the quantities are same as in Fig. 8.

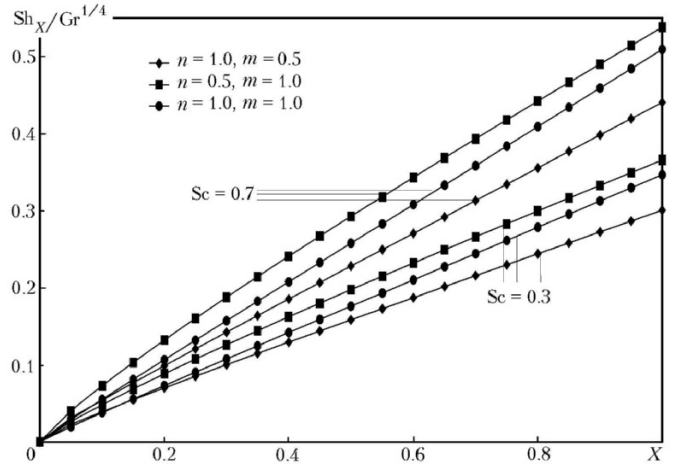


Fig. 10. Local Sherwood number for different values of Sc, $n$, and $m$. The values of the quantities are same as in Fig. 8.

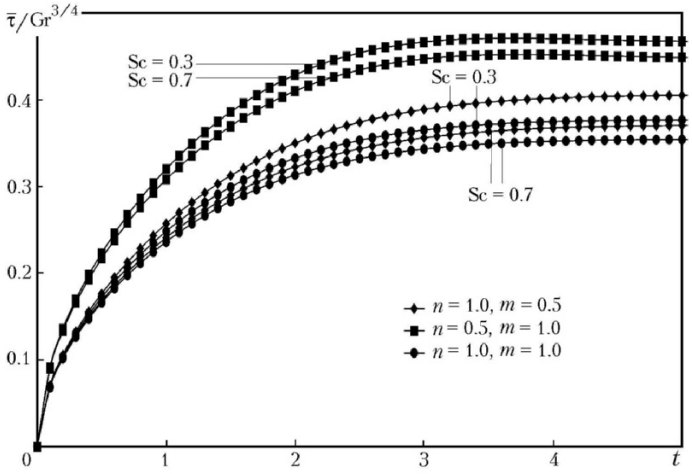


Fig. 11. Average skin friction for different values of Sc, $n$, and $m$. The values of the quantities are same as in Fig. 8.

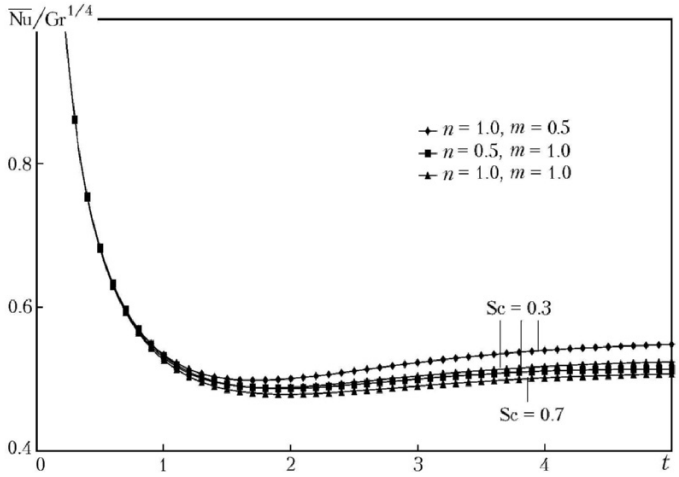


Fig. 12. Average Nusselt number for different values of Sc, $n$, and $m$. The values of the quantities are same as in Fig. 8.

In Fig. 4, transient concentration profiles are plotted for different values of $m$ and $\phi$. It is observed that the concentration behaves as the temperature. Here no temporal maximum is observed. As expected, the concentration is lower for systems with larger values of $\phi$ or $m$. It is also shown that when $m > n$, a steady-state value is reached more rapidly in comparison to the case of $n = m$, but when $m < n$, a steady-state value is reached more slowly.

Steady-state velocity, temperature, and concentration profiles for various Schmidt and Prandtl numbers are plotted in Figs. 5–7. It is seen that the rate of mass transfer increases as the Schmidt number decreases. The same is true for the rate of heat transfer relative to the Prandtl number. Hence, a decrease in the Schmidt number or Prandtl number leads to an increase in the maximum velocity for fixed values of other parameters. The temperature increases with the Schmidt number and the concentration increases with the Prandtl number, which one might expect. The thermal boundary layer decreases for a larger value of Pr. Steady-state concentration profiles are attained earlier for lower Pr.

The effects of Sc, $n$, and $m$ on the local skin friction, Nusselt number, and Sherwood number are shown in Figs. 8–10. The local wall shear stress decreases as $n$ or $m$ increases and increases with decreasing value of Sc due to the increase in the velocity, as shown in Fig. 5. The local Nusselt number increases with decreasing value of either Sc or $m$, whereas it increases with n. This trend is just opposite to the variation of the local Sherwood number with Sc, $n$, and $m$.

Time dependences of the average values of skin friction, Nusselt number, and Sherwood number for various parameters are given in Figs. 11–13. The average skin friction increases at small values of $t$, whereas at large $t$ it is

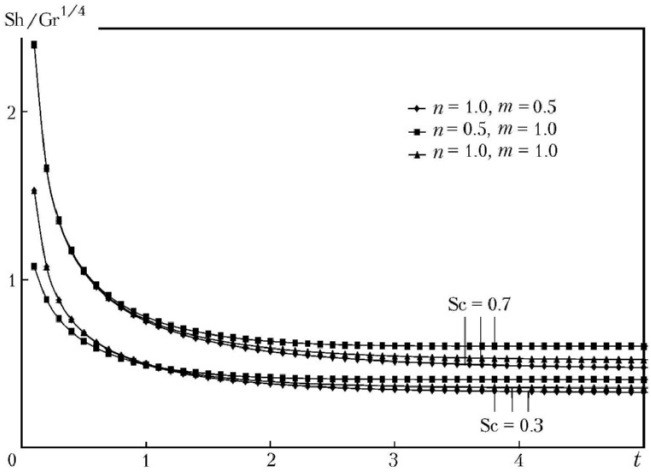


Fig. 13. Average Sherwood number for different values of Sc, $n$, and $m$. The values of the quantities are same as in Fig. 8.

independent of $t$. The average skin friction is reduced with increase in each of the values of Sc, $n$, and $m$ throughout the transient period. From Fig. 12 we conclude that the average Nusselt number decreases sharply at small values of $t$, being unaffected by Sc, $n$, and $m$, but at large values of $t$ Nu it is independent of time. The average Nusselt number has the same trend with respect to Sc as the average skin friction. An increase in the value of $n$ leads to an increase in the average Nusselt number, but to a decrease in the average Sherwood number. The inverse situation takes place for a change in the value of $m$. We observe from Fig. 13 that the behavior of the average Sherwood number with respect to Sc is the same as for local Sherwood number. The average Sherwood number is independent of time for large $t$.

## CONCLUSIONS

1. Velocity decreases with increasing value of exponents $n$ and $m$.
2. The effect of $n$ on velocity is more pronounced than that of $m$.
3. A lower temperature is observed for a system with a higher value of exponent $n$.
4. No temporal maximum is observed for concentration.
5. Steady state is reached very slowly when $m < n$.
6. The local wall shear stress decreases as either $n$ or $m$ increases.
7. Variations of the local Nusselt number and Sherwood number are opposite with respect to Sc, $n$, and $m$.
8. An increase in the value of $m$ leads to a decrease in the average Nusselt number, but to an increase in the average Sherwood number.

## NOTATION

$a$ and $b$, constants; $C'$, species concentration; $C$, dimensionless species concentration; $D$, coefficient of diffusion in the mixture; Gc, mass Grashof number; Gr, thermal Grashof number; $g$, acceleration due to gravity; $L$, reference length; $m$, exponent in power law for mass flux variation; $n$, exponent in power law for surface temperature variation; $N$, buoyancy ratio parameter; $\overline{\mathrm{Nu}}$, average Nusselt number; $\mathrm{Nu}_X$, local Nusselt number; Pr, Prandtl number; $q_w$, mass flux; Sc, Schmidt number; $\overline{\mathrm{Sh}}$, average Sherwood number; $\mathrm{Sh}_X$, local Sherwood number; $T'$, temperature; $T$, dimensionless temperature; $t'$, time; $t$, dimensionless time; $u$ and $v$, velocity components in $x$ and $y$ directions, respectively; $U$ and $V$, dimensionless velocity components in $X$ and $Y$ directions; $x$, spatial coordinate along the plate; $X$, dimensionless longitudinal coordinate; $y$, spatial coordinate along upward normal to the plate; $Y$, dimensionless normal coordinate; $\alpha$, thermal diffusivity; $\beta$, volumetric coefficient of thermal expansion; $\beta^*$, volumetric coefficient of expansion with concentration; $\phi$, angle of inclination of the plate with horizontal; $\nu$, kinematic viscosity; $\tau_X$, dimensionless local skin friction; $\bar{\tau}$, dimensionless average skin friction. Subscripts: w, on the wall; $\infty$, free stream conditions.

## REFERENCES


1. E. V. Somers, Theoretical considerations of combined thermal and mass transfer from a vertical flat plate, *J. Appl. Mech.*, **23**, 295–301 (1956).
2. W. R. Wilcox, Simultaneous heat and mass transfer in free convection, *Chem. Eng. Sci.*, **13**, 113–119 (1961).
3. B. Carnahan, H. A. Luther H.A., and J. O. Wilkes, *Applied Numerical Methods*, John Wiley and Sons, New York (1969).
4. B. Gebhart and L. Pera, The nature of vertical natural convection flows resulting from the combined buoyancy effects of thermal and mass diffusion, *Int. J. Heat Mass Transfer*, **14**, 2025–2050 (1971).
5. G. D. Callahan and W. J. Marner, Transient free convection with mass transfer on an isothermal vertical flat plate, *Int. J. Heat Mass Transfer*, **19**, 165–174 (1976).
6. V. M. Soundalgekar and P. Ganesan, Transient free convection with mass transfer on a vertical plate with constant heat flux, Energy Research, **9**, 1–17 (1985).
7. G. Palani and Kwang-Yong Kim, The effects of MHD on free-convection flow past a semi-infinite isothermal inclined plate, *J. Eng. Phys. Thermophys.*, **8**1, No. 4, 724–731 (2008).
8. K. Ekambavannan and P. Ganesan, Finite difference analysis of unsteady natural convection flow along an inclined plate with variable surface temperature and mass diffusion, *Wärme and Stoffübertragung*, **31**, 17–24 (1995).